Modified sine-Gordon theory with static multikinks

Chris Halcrow[*]
Department of Physics, KTH-Royal Institute of Technology, SE-10691, Stockholm, Sweden

Renjan Rajan John[†]
School of Pure and Applied Physics, Mahatma Gandhi University, Kottayam, Kerala 686 560, India

Anusree N.[‡]
Department of Physics, Sree Narayana College, Kannur, Kannur University, Kerala 670 007, India

(Received 11 December 2023; revised 6 February 2024; accepted 20 August 2024; published 13 September 2024)

We construct a modified non-Bogomol'nyi-Prasad-Sommerfield sine-Gordon theory which supports stable static kinks of arbitrary topological degree N. We use this toy model to study problems that are interesting for higher-dimensional soliton theories supporting multisolitons. We construct a 2-kink collective coordinate model and use it to generate scattering trajectories, which are compared to full-field dynamics. We find that the approximation works well, but starts to fail as radiation becomes more important, due to our model becoming less Bogomol'nyi-Prasad-Sommerfield or when the initial kink velocities are large. We also construct the quantum 2-kink using various approximations and consider how these quantum corrections affect the binding energy of the 2-kink.

DOI: 10.1103/PhysRevD.110.065010

I. INTRODUCTION

Kinks are solitons in one dimension. They are most often used as toy models for solitons in more complicated, higher-dimensional theories. In fact, it was Skyrme who derived the sine-Gordon model as "a simplified model" of the Skyrme model [1] and thoroughly studied its kink solution, interpreted as particles [2] (the sine-Gordon model had previously been used in the study of surfaces with constant negative curvature and crystal dislocations). Since then authors have studied more models and their kink solutions, dynamics, and quantum corrections to their masses.

In this paper, we will construct a modified sine-Gordon theory which supports multikinks. Here, we define a multikink as a static solution that can be continuously deformed into multiple well-separated 1-kinks, each a solution to the equations of motion. Static multikinks have been seen in a 1D (one-dimensional) theory on a nontrivial background geometry [3]. However, the geometry breaks translation symmetry meaning that there is no *solution* that can be interpreted as widely separated kinks. Many soliton theories are BPS (Bogomol'nyi-Prasad-Sommerfield), meaning that solutions satisfy a first-order differential equation and have no binding energy. Our theory is non-BPS. In the following paragraphs, we argue why these non-BPS kinks can serve as better toy models for solitons in higher-dimensional theories than BPS kinks.

In higher dimensions, multisolitons are often the most interesting part of the theory. For example, there is a rich landscape of static multiskyrmion [4] and monopole solutions [5]. All known one-component kink models satisfy the BPS property [6], and these theories cannot support static stable multikinks. Hence a BPS kink theory cannot be used as a toy model for problems involving multisolitons since they do not support static multikinks. The attractive interaction of separated solitons is vital to understanding these multisolitons, as well as the stability and structure of vortex and skyrmion lattices, which appear in condensed matter theory [7,8]. However, the interaction of BPS kinks is repulsive (e.g., sine-Gordon). There can be attractive dynamics, but only between a kink and an antikink, whose dynamics will be very different than two kinks.

Another major idea in soliton theory is the collective coordinate approximation, first introduced by Manton for vortex scattering [9]. Here one constructs a manifold of configurations, sometimes called the configuration space, parametrized by the "collective coordinates" of the solitons (e.g., their positions). The manifold has a metric and potential induced by the field theory. Soliton dynamics are then

[*]Contact author: chalcrow@kth.se
[†]Contact author: renjan@mgu.ac.in
[‡]Contact author: anusreekanakaraj@gmail.com

described as geodesics on the manifold, crucially depending on the metric and potential. These have been constructed for integrable models such as critically coupled vortices [10,11], monopoles [12], and instantons [13]. However, the problem is more complicated for non-BPS theories: there is usually not a canonical choice of collective coordinates and so there are ambiguities in the definition of the configuration space. This ambiguity means there are many different ideas for how to construct CCMs such as the inclusion of shape modes [14], mechanization [15], perturbative approaches [16], projecting instanton solutions [17], pinning [18], and gradient decent curves [19–21]. However, all these studies concern BPS models, or the interaction of kinks with antikinks—not kink-kink dynamics. Constructing collective models for non-BPS multilink scattering may help one understand how to do this systematically for soliton-soliton interactions in higher-dimensional models.

There is also significant debate about soliton binding energies. Many papers are motivated to solve the "binding energy problem" in the Skyrme model: that the classical binding energy of Skyrmions is larger than the binding energy of nuclei by an order of magnitude [22–24]. However, it has been argued that the classical binding energy is not a good measure of the quantum binding energy. Loop corrections [25] and the inclusion of "vibrational modes" [26] greatly affect skyrmion masses, and have been argued to solve the binding energy problem without using a carefully tuned model, but these ideas require further testing. BPS kink models cannot give much intuition about this problem since their classical binding energies vanish, and there is no multikink with a binding energy to measure.

There is a clear need to develop non-BPS kink theories which can serve as toy models for the physically interesting non-BPS models in higher dimensions. Recently one such model has been constructed and studied [27], which has also been studied with different motivations [28,29]. This is a two-component theory in which kinks attract at long range but repel at short range. Thus there can be static, stable multikinks. However, this model only supports up to two kinks.

In this paper, we introduce a kink theory that supports stable kinks with arbitrary charge N, mimicking higher-dimensional theories. Our model is a modified version of sine-Gordon theory. We will study the static solutions, create a collective coordinate model for 2-kink dynamics, and quantize this using various approximation. Throughout, we try to answer the questions one would ask about higher-dimensional theories, focusing on the validity of the collective coordinate approximation and binding energies. The broad range of topics that we cover shows the large number of questions one can ask about this new type of kink model.

II. STABLE STATIC MULTIKINK SOLUTIONS

We begin by briefly reviewing [27], which details the interaction between kinks. Consider a multicomponent scalar theory with Lagrangian

$$\begin{aligned}\mathcal{L} &= \frac{1}{2}\partial_\mu \Phi_a \partial^\mu \Phi_a - V(\Phi_a) \\ &= \frac{1}{2}\dot{\Phi}_a\dot{\Phi}_a - \frac{1}{2}\partial_x\Phi_a\partial_x\Phi_a - V(\Phi_a). \end{aligned} \tag{1}$$

We will assume that the potential has N minima which we can enumerate. A 1-kink is a static solution of the equations of motion that joins two adjacent minima of the potential. Due to the translational symmetry of $\mathcal{L}$, the kink can be translated. Hence, if we define a base-point configuration with position $X = 0$, $\Phi^0(x)$, we can define a kink with position X as $\Phi^X(x) = \Phi^0(x - X)$.

Consider a single kink which approaches the vacuum Φ^{v_0} as $x \to \infty$. Near the vacuum, we can Taylor expand

$$\Phi(x) = \Phi^{v_0} + \boldsymbol{\phi}(x). \tag{2}$$

The tail $\phi_a(x)$ satisfies the Euler-Lagrange equation

$$\partial_x^2\phi_a - \partial_a\partial_b V(\Phi^{v_0})\phi_b = 0. \tag{3}$$

The solution to this equation is given in terms of the eigenvalues λ_n and eigenvectors $\boldsymbol{\mu}_n$ of the Hessian $\partial_a\partial_b V(\Phi^{v_0})$,

$$\boldsymbol{\phi} = \sum_n a_n \boldsymbol{\mu}_n e^{-\sqrt{\lambda_n}x}. \tag{4}$$

Now consider two well-separated kinks with positions $+X$ and $-X$, denoted by Φ^{+X} and Φ^{-X}, respectively. Suppose that the two kinks relate three adjacent vacua such that they share one vacuum Φ^{v_0}. A superposition of the kinks is given by

$$\Phi(x) = \Phi^{-X}(x) + \Phi^{+X}(x) - \Phi^{v_0}. \tag{5}$$

If X is large, this can be written as

$$\begin{aligned}\Phi(x) &\approx \Phi^{-X}(x) + \phi^{+X}(x) - \Phi^{v_0}, \qquad x \ll 0, \\ \Phi(x) &\approx \Phi^{+X}(x) + \phi^{-X}(x) - \Phi^{v_0}, \qquad x \gg 0. \end{aligned} \tag{6}$$

One can then evaluate the static energy of the theory to find the interaction of the two kinks [27]. It is

$$E^{\text{interaction}}(\Phi) = (\partial_x\phi_a^{-X}\phi_a^X - \partial_x\phi_a^X\phi_a^{-X})|_{x=0}. \tag{7}$$

Thus the interaction energy depends only on the tail configurations at the center-of-mass of the two kinks. This type of argument was first given for planar skyrmion [30], and has since been used for three-dimensional [31] and magnetic [32] skyrmions.

Using (7) one can show that ϕ^4, ϕ^6, and sine-Gordon kinks repel, while kinks and antikinks attract. More generally, in one-component scalar field theories, a kink-kink will repel while an antikink-kink will attract and

annihilate. As a result, static 2-kink solutions had not been considered until recently. The basic idea in [27] was to construct solutions which act like a kink-kink in one component and an antikink-kink in another. One component provides repulsion and the other attraction. If these are balanced, a static stable 2-kink can exist.

III. MODIFIED SINE-GORDON THEORY

In [27,29] a modified ϕ^4 theory which could support up to two kinks was constructed. However, most higher-dimensional soliton theories of interest support an arbitrary number of kinks. To mimic this feature, we will now develop a modified sine-Gordon theory. The new feature of this model compared to other modified sine-Gordon theories [33–35] is the existence of stable, static multikink solutions. Their existence relies crucially on the fact that our model contains more than one field. We will consider the simplest nontrivial case of a two-component theory.

The theory has a Lagrangian of the form (1). We searched for a modified form of the sine-Gordon potential with an infinite number of discrete vacua and a Hessian that is equal at all vacua. A simple theory that obeys these requirements is

$$\tilde{\mathcal{L}} = \frac{1}{2}\partial_{\tilde{t}}\tilde{\Phi}_a\partial_{\tilde{t}}\tilde{\Phi}_a - \frac{1}{2}\partial_{\tilde{x}}\tilde{\Phi}_a\partial_{\tilde{x}}\tilde{\Phi}_a - \frac{m^2}{\beta^2}(1-\cos\beta\tilde{\Phi}_1) - \frac{\mu_1^2 m^2}{8\beta^2}\left(1-\frac{2\beta\tilde{\Phi}_2}{\mu_2}-\cos\left(\frac{\beta\tilde{\Phi}_1}{2}\right)\right)^2. \tag{8}$$

Throughout the text, we have denoted dimensionful units with a tilde. Here, we have used units where $c=1$. The parameters m and β^2 have dimensions of mass and inverse mass times length, respectively, while μ_1 and μ_2 are dimensionless. The Lagrangian (8) reduces to sine-Gordon theory when $\mu_1 = 0$. We can now define $\Phi = \beta\tilde{\Phi}$, $t = m\tilde{t}$, and $x = m\tilde{x}$ to factor out many of the theories' parameters. The dimensionless Lagrangian $\mathcal{L}$ is defined implicitly by

$$\tilde{\mathcal{L}} = \frac{m}{\beta^2}\mathcal{L} \equiv \frac{m}{\beta^2}\left[\frac{1}{2}\dot{\Phi}_a\dot{\Phi}_a - \frac{1}{2}\partial_x\Phi_a\partial_x\Phi_a - (1-\cos\Phi_1) - \frac{\mu_1^2}{8}\left(1-\frac{2\Phi_2}{\mu_2}-\cos\left(\frac{\Phi_1}{2}\right)\right)^2\right], \tag{9}$$

revealing that in the new units, the classical equations of motion are independent of β and m. The classical numerical results in this paper will be presented for the case where $m/\beta^2 = 1$.

The potential $V(\Phi)$ contained in $\mathcal{L}$ (9) admits two countably infinite sets of discrete vacua, given by

$$(\Phi_1,\Phi_2) = (4n\pi, 0) \quad \text{and}$$
$$(\Phi_1,\Phi_2) = (2(2n+1)\pi, \mu_2), \quad \text{where } n\in\mathbb{Z}. \tag{10}$$

Define $\mathcal{V}$ as the set of all vacua. The topological classification of 1D theories is due to the zeroth homotopy group of the vacuum manifold, $\pi_0(\mathcal{V})$ [[36], Chapter 4]. In our case, this is simply the set of vacua, isomorphic to $\mathbb{Z}$. Since the values in $\mathcal{V}$ can be ordered by the Φ_1 coordinate, we can unambiguously define a topological charge of a solution as the difference between its initial and final Φ_1 values. We normalize this value by dividing by 2π. Hence we define an N-kink as the minimal energy solution which interpolates between $\Phi_1 = 2\pi n$ and $\Phi_1 = 2\pi(n+N)$. Without loss of generality, we can set $n=0$ and we do so for the rest of the paper, defining the base point for the homotopy group. We further define the location of the kinks by the preimage of the point halfway between the boundary values.

First, consider a 1-kink, which interpolates between $(\Phi_1,\Phi_2) = (0,0)$ and $(\Phi_1,\Phi_2) = (2\pi,\mu_2)$. The tail of the kink decays exponentially at a rate determined by the Hessian at the vacua (4). The Hessian is equal at all vacua and is given by

$$\left.\frac{\partial^2 V}{\partial\Phi_a\partial\Phi_b}\right|_{\Phi=(2\pi,m)} = \begin{pmatrix} 1 & 0 \\ 0 & \mu_1^2/\mu_2^2 \end{pmatrix}. \tag{11}$$

Hence the kink decays as

$$(\phi_1,\phi_2) \sim (ae^{-|x|}, be^{-\mu_1|x|/\mu_2}), \tag{12}$$

as x tends to $\pm\infty$.

Now consider the kink-kink interaction where the first kink interpolates between (0,0) and $(2\pi,m)$ and has position $-X$, while the second kink interpolates between $(2\pi,m)$ and $(4\pi,0)$ and has position X. The interaction energy again depends on the Hessian and is given by (7)

$$E^{\text{int}} = a^2e^{-2X} - b^2\frac{\mu_1}{\mu_2}e^{-2\frac{\mu_1}{\mu_2}X}. \tag{13}$$

The form of the interaction energy reveals that there are competing attractive and repulsive forces, depending on the parameters μ_1 and μ_2. Hence we can expect a stable 2-kink, at least in some parameter range. Since the Hessian is equal at all vacua, the calculation is almost identical if we consider the interaction between a 2-kink and a 1-kink. The only difference is in the coefficients a and b. As such, we expect that if there is a stable 2-kink, there will be a stable 3-kink, and so on.

To find N-kink solutions, we use numerics. For simplicity, we use a gradient flow algorithm to find the energy minimizing N-kink. First, consider the 1- and 2-kinks. We implemented the gradient flow on a grid of 400 points with lattice spacing 0.126 using Python. We considered the following as an initial guess for the 2-kink solution:

$$\Phi_1 = \pi(2+\tanh(x+X)+\tanh(x-X)),$$
$$\Phi_2 = \mu_2 e^{-x^2}. \tag{14}$$

With the parameters $\mu_1 = 2$, $\mu_2 = 6.1$, the energy of the 1-kink was found to be $E_1 = 10.24$, whereas the 2-kink has energy $E_2 = 19.44$. Hence the 2-kink is energetically favored over two 1-kinks. The percentage binding energy per soliton is

$$E_{\text{bind}} = \frac{2E_1 - E_2}{2E_1} \times 100\% = 5.1\%. \tag{15}$$

One feature of BPS theories is that E_{bind} vanishes. The fact ours is nonzero confirms that our theory is non-BPS. The binding energy depends on the parameters m and μ. We find this dependence and plot it in Fig. 1. The plot can be used to choose the parameters to generate a model with the desired binding energy. Later we will study a variety of models, including the model with $\mu_1 = 2$, $\mu_2 = 4$. This is much closer to BPS with a percentage binding energy per soliton of only 0.8%.

There are also stable kinks for larger N. The 1-, 2-, 3-, 4- and 8-charge kinks are displayed in Fig. 2. We see that the even and odd charge kinks are either odd (with a shift) or even in Φ_2. We plot the fields $\Phi_a(x)$ (top) and also plot these on the potential landscape (bottom).

There is also an infinite charge kink, equivalent to a periodic solution on a circle. There are many examples of solitons on a background where one direction is a circle, such as calorons [37], planar skyrmions [38], and monopoles [39]. We can calculate the solution by putting the model on a circle of length L and using shifted periodic boundary conditions. These are

$$\Phi_1(0) = 0, \qquad \Phi_2{}'(0) = 0, \tag{16}$$

$$\Phi_1(L) = 2\pi, \qquad \Phi_2{}'(L) = 0. \tag{17}$$

We then vary over L to find the minimum energy chain. Our method is to solve the model repeatedly using the same lattice spacing, but a different number of points. We then find the L which minimizes the energy. The energy as a

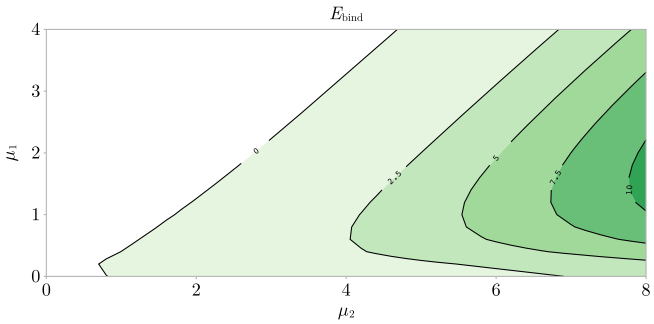

FIG. 1. The percentage binding energy per kink for the 2-kink as a function of μ_1 and μ_2.

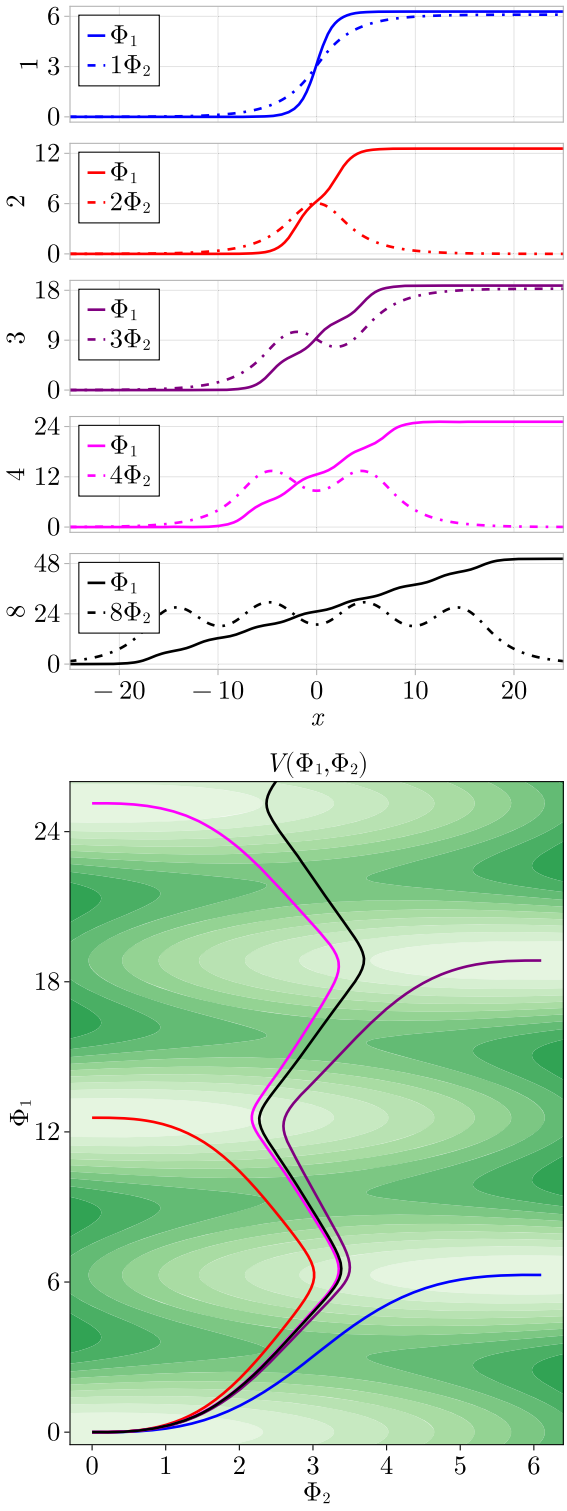

FIG. 2. Plots of the 1-, 2-, 3-, 4- and 8-charge kinks for $\mu_1 = 2$, $\mu_2 = 6.1$, displayed in blue, red, purple, magenta, and black, respectively. These are plotted as functions of x (top) and on the target space (bottom). Light/dark green corresponds to a smaller/larger potential energy. The N-kink joins a point with $\Phi_1 = 0$ to a point with $\Phi_1 = 2\pi N$.

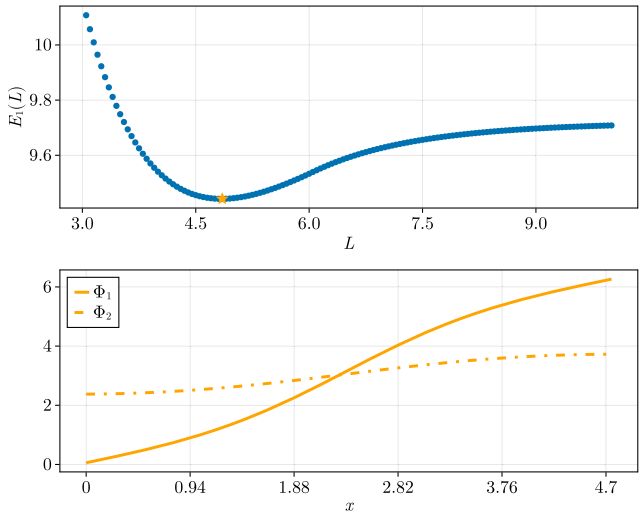

FIG. 3. The periodic kink for $\mu_1 = 2$, $\mu_2 = 6.1$. The energy of the 1-kink as a function of box size L (top) and a plot of the optimal shifted-periodic solution (bottom).

function of L, and the minimal energy solution are shown in Fig. 3. The chain is related to the finite kink solutions. Note that configuration in Fig. 3 satisfies $\Phi_2'(0) = 0$, like the even N-kinks. So this chain solution is the large N limit for even N-kinks. The odd N-kinks satisfy $\Phi_2(0) = \mu_2/2$. Their large N limit is equal to the chain in Fig. 3 shifted by a half unit cell. So the infinite chain limit is different for odd and even N, but since the limit is just the same solution translated, they have the same energy.

The classical percentage binding energy per kink of an N-kink is given by the formula

$$E_{\text{bind}}(N) = \frac{NE_1 - E_N}{NE_1}. \tag{18}$$

This is an important quantity in the Skyrme model, where the formula gives the classical binding energy of nuclei per nucleon. We calculate this value for $N = 1$–20 in our model, and plot it in Fig. 4. Similar to nuclei, kink binding energies asymptote to a constant value, in this case 7.8%. We fit points to a polynomial decay and find that the classical binding energy per kink goes as $1/N$.

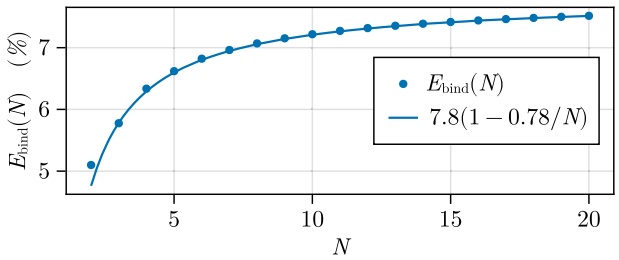

FIG. 4. The percentage binding energy per kink, for $N = 1$–20, for $\mu_1 = 2$ and $\mu_2 = 6.1$.

IV. COLLECTIVE COORDINATE MODEL

A. Making the model

In this section we construct a one-dimensional collective coordinate model (CCM) for two kinks, in which we use the kink positions $\pm X$ as the modulus. In dimensionful units, the CCM is described by a Lagrangian of the form

$$L = \frac{1}{2}\tilde{g}_{\tilde{X}\tilde{X}}(\tilde{X})\dot{\tilde{X}}^2 - \tilde{U}(\tilde{X}), \tag{19}$$

where the metric $\tilde{g}_{\tilde{X}\tilde{X}}$ on the one-dimensional moduli space is

$$\tilde{g}_{\tilde{X}\tilde{X}}(\tilde{X}) = \int_{-\infty}^{\infty}\left[\left(\frac{\partial\tilde{\Phi}_1}{\partial\tilde{X}}\right)^2 + \left(\frac{\partial\tilde{\Phi}_2}{\partial\tilde{X}}\right)^2\right]d\tilde{x} \tag{20}$$

and the potential $\tilde{U}(\tilde{X})$ is

$$\tilde{U}(\tilde{X}) = \tag{21}$$

$$\int_{-\infty}^{\infty}\left(\frac{1}{2}\left(\frac{\partial\tilde{\Phi}_1}{\partial\tilde{x}}\right)^2 + \frac{1}{2}\left(\frac{\partial\tilde{\Phi}_2}{\partial\tilde{x}}\right)^2 + \frac{m^2}{\beta^2}V(\beta\tilde{\Phi})\right)d\tilde{x}. \tag{22}$$

As in the previous section, we can switch to new units $x = m\tilde{x}, X = m\tilde{X}, \Phi = \beta\tilde{\Phi}$ to find the dimensionless Lagrangian

$$L = \frac{1}{2}g_{XX}(X)\dot{X}^2 - U(X), \tag{23}$$

where, using (20) and (21),

$$\tilde{g}_{\tilde{X}\tilde{X}}(\tilde{X}) = \frac{m}{\beta^2}g_{XX}(X), \qquad \tilde{U}(\tilde{X}) = \frac{m}{\beta^2}U(X). \tag{24}$$

We'll consider the dynamics of the dimensionless theory (23) for the rest of this section.

Let us again consider two 1-kinks, one that interpolates from (0,0) to $(2\pi, \mu_2)$ and another that interpolates from $(2\pi, \mu_2)$ to $(4\pi, 0)$. We define the position of these kinks X and $-X$ as the preimage where the first component takes value at the midpoint, i.e., we pin the position of the kinks to X and $-X$ such that

$$\Phi_1(-X) = \pi, \qquad \Phi_1(X) = 3\pi. \tag{25}$$

For a given separation $2X$ between the two kinks, we obtained the configuration (Φ_1, Φ_2) that minimizes the energy (21) using gradient flow. We again implemented the flow on a grid with 400 points and lattice spacing 0.126 and used the configuration in (14) as our initial guess. We did this for $0.5 < X < 13$ with X fixed at each x lattice point, generating around one hundred configurations for the model. This generates the configuration space, parametrized by $\Phi(x, X)$. We used the central difference method to

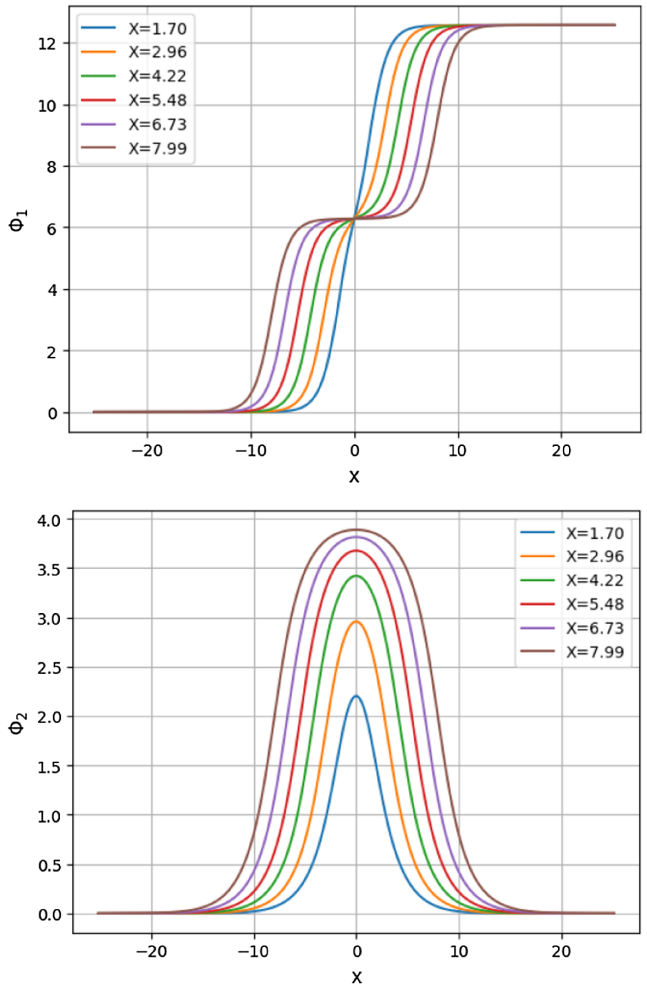

FIG. 5. Energy minimising Φ_1 (top) and Φ_2 (bottom) for different values of X, for $\mu_1 = 2$ and $\mu_2 = 4$.

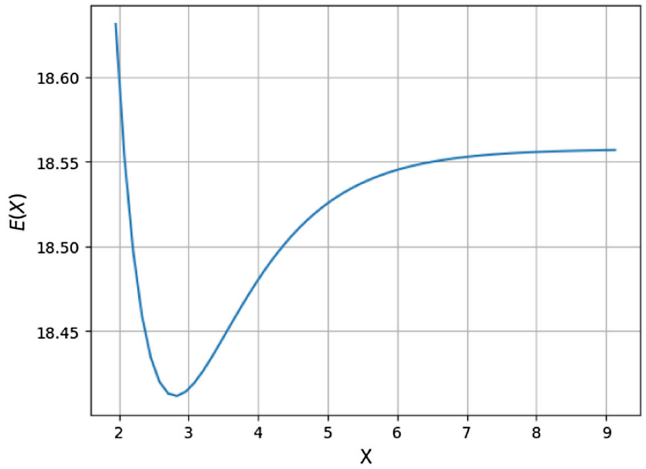

FIG. 6. Energy as a function of X for $\mu_1 = 2$ and $\mu_2 = 4$.

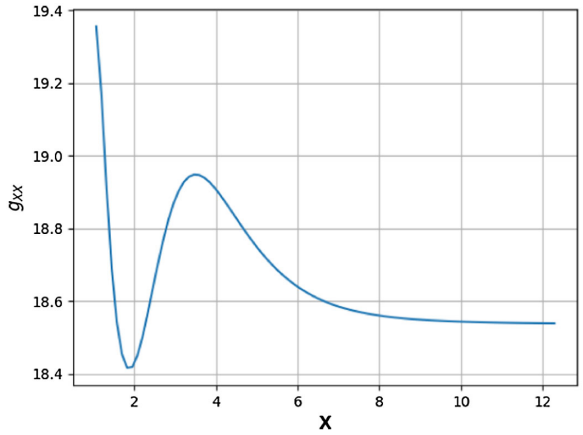

FIG. 7. Metric g_{XX} as a function of X for $\mu_1 = 2$ and $\mu_2 = 4$.

calculate the derivatives of Φ with respect to both the kink position X and the spatial coordinate x in (20) and (21).

Several configurations for different X are plotted in Fig. 5. The resulting energy of these configurations as a function of the separation is plotted in Fig. 6. We see that the energy as a function of the separation has a minimum at a finite nonzero X, agreeing with the field theory expectation that the 2-kink is energetically favored over two 1-kinks. The energy increases sharply when the kinks are brought closer together, but only increases slowly as they are moved further apart. The metric is plotted in Fig. 7 and has two critical points.

B. Kink dynamics

Our collective coordinate model can be used to simulate kink-kink dynamics. We will first study the full-field time evolution of the kinks by solving the equations of motion in the field theory. We will then go on to see how well these are modeled by our CCM.

The full-field dynamics is given by the Euler-Lagrange equation of motion that follows from (1)

$$\ddot{\Phi}_a = \frac{\partial^2 \Phi_a}{\partial x^2} - \frac{\partial V}{\partial \Phi_a}. \tag{26}$$

To solve this, we introduce the field velocity Ψ,

$$\dot{\Phi}_a = \Psi_a \tag{27}$$

$$\dot{\Psi}_a = \frac{\partial^2 \Phi_a}{\partial x^2} - \frac{\partial V}{\partial \Phi_a}. \tag{28}$$

We solve these numerically using the Leapfrog method. We update Φ and Ψ as follows:

$$\Phi_{n+1} = \Phi_n + \Psi_n dt + \frac{1}{2} b_n dt^2, \tag{29}$$

$$\Psi_{n+1} = \Psi_n + \frac{1}{2}(b_n + b_{n+1}) dt, \tag{30}$$

where

$$b_n = \frac{\partial^2 \Phi_n}{\partial x^2} - \frac{\partial V_n}{\partial \Phi_n}. \tag{31}$$

From the time evolution of Φ, we obtain the time evolution of X using (25). The initial velocity field is generated by

$$\Psi_0(x) = \frac{\partial}{\partial t}\Phi(X - vt, x)|_{t=0} = -v\frac{\partial \Phi(X,x)}{\partial X}. \tag{32}$$

In the collective coordinate approximation, dynamics is dictated by the equation of motion that follows from (23),

$$\ddot{X} + \frac{1}{2g}((\partial_X g(X))\dot{X}^2 + 2\partial_X U(X)) = 0. \tag{33}$$

To solve this, we introduce $v = \dot{X}$. The equations become

$$\dot{X} = v \tag{34}$$

$$\dot{v} = -\frac{1}{2g}((\partial_X g)v^2 + 2\partial_X U). \tag{35}$$

Starting with the initial data, $(X, v) = (X_0, v_0)$, we evolve these equations numerically using the Leapfrog method, updating X and v as follows:

$$X_{n+1} = X_n + v_n dt + \frac{1}{2}a_n dt^2 \tag{36}$$

$$v_{n+1} = v_n + \frac{1}{2}(a_n + a_{n+1})dt \tag{37}$$

where

$$a_n = -\frac{1}{2g}((\partial_X g(X_n))v_n^2 + 2\partial_X U(X_n)). \tag{38}$$

Here the derivatives of the metric g_{XX} and the potential U with respect to the kink position X are calculated using a cubic spline.

We now generate $X(t)$, obtained from the CCM as well as from the full-field theory for different values of initial velocity. We first consider trajectories where $X(0) = 8$ and $v = 0.02, 0.2$. We interrupt the dynamics when $X(t) > 8$ in the CCM. The results are plotted in Figs. 8 and 9 for the model with parameters $\mu_1 = 2$ and $\mu_2 = 4$. This model is close to the BPS model, and we obtain a very good approximation for small velocities, with the approximation becoming worse as we increase the velocity. This is expected. As the configuration passes through the minimum of the potential, there is a large energy transfer from potential to kinetic energy and back again. In the full-field theory, the 2-kink can radiate, losing energy. Hence the outgoing kinks have a phase shift and are slower than the incoming kinks. In the collective coordinate model, the kink cannot radiate and the outgoing kinks have the same velocity as the incoming ones.

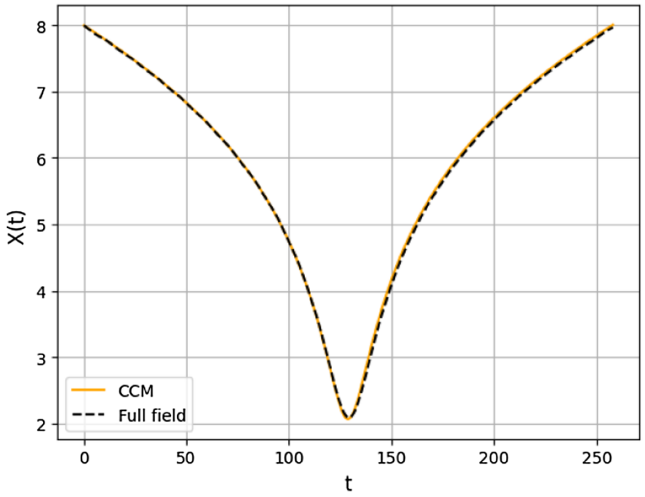

FIG. 8. $X(t)$ for initial velocity $v = 0.02$ and initial position 8 for $\mu_1 = 2$ and $\mu_2 = 4$.

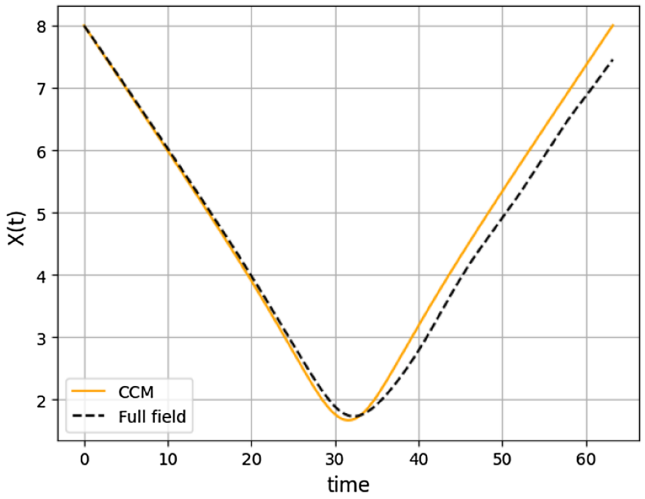

FIG. 9. $X(t)$ for initial velocity $v = 0.2$ and initial position 8 for $\mu_1 = 2$ and $\mu_2 = 4$.

The approximation appears to break down when we move away from near-BPS models. In Fig. 10 we consider the parameters $\mu_1 = 2$ and $\mu_2 = 6.1$. We display this for a longer time than the other plots, to better understand the behavior of the field theory. At large t, the approximation becomes a lot less accurate. Note that the "meson" mass in the second field is μ_1/μ_2 so that as μ_2 increases, it costs less and less energy to excite radiation. Hence radiation becomes more important as m increases. Here, the two kinks radiate their kinetic energy away and cannot escape from the potential well. Again, since the CCM cannot radiate, it cannot model this behavior. Hence the CCM does not capture this main qualitative feature of the dynamics.

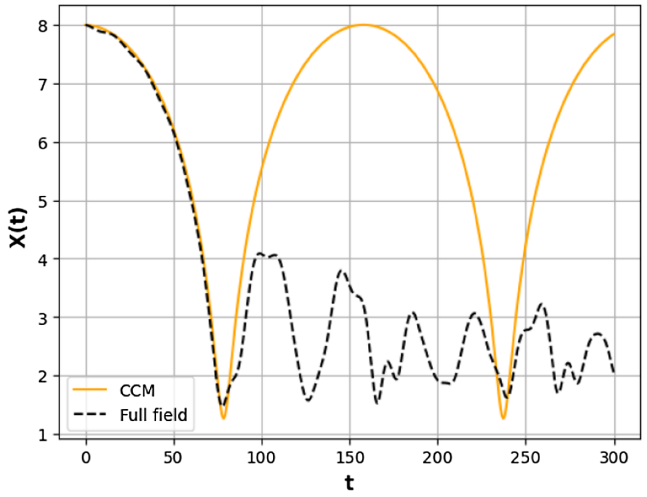

FIG. 10. $X(t)$ for initial velocity $v = 0.01$ and initial position 8 for $\mu_1 = 2$ and $\mu_2 = 6.1$.

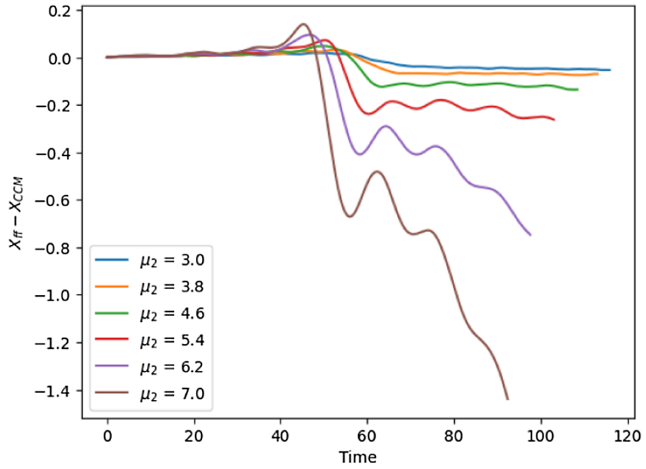

FIG. 11. The difference between the full-field calculation $X_{ff}(t)$ and the collective coordinate model $X_{CCM}(t)$ in the case $X(0) = 8$, $v = 0.1$ for $\mu_1 = 2$ and a variety of μ_2.

However, note that the model does capture the correct behavior until the 2-kink approaches the bottom of the potential. Thus the model does seem to capture the potential and curvature of the configuration space. Hence it might not be our model that fails, but the geodesic approximation itself. The approximation should fail when velocities and radiation are high, so it makes sense that it fails when the kinks are at the bottom of the potential well, where their velocity is maximal. Another possibility is that our CCM model is too simple. Other authors have considered CCMs with multiple collective coordinates, one which usually describes an internal shape mode of the kinks [14,16]. We could extend our model by including this shape mode for one or each of the kinks, and see if the approximation becomes significantly better.

The geodesic approximation relies on two assumptions: that the velocity (and hence energy transfer to radiation) is small and that the theory is close to BPS. We now probe the second of these assumptions in more detail. Consider the scattering of two kinks with initial positions $X = 8$ and $X = -8$ with velocity $v = 0.1$, the model parameters $\mu_1 = 2$ fixed and μ_2 varying. We construct the CCM, simulate the CCM dynamics and the full-field dynamics for a variety of μ_2. As μ_2 increases we move further from a BPS theory. The difference between CCM and full-field dynamics for the various models are plotted in Fig. 11. We see that for $\mu_2 < 5.4$ the CCM captures the main features of the model: although a large error is generated as the model passes near the bottom of the potential, the outgoing kinks have approximately constant velocity, and the error remains approximately constant after the bounce. However, when $\mu_2 > 5.4$ the qualitative behavior changes: this is when the 2-kink gets trapped in the potential well, as seen in Fig. 10.

Overall, we have successfully constructed collective coordinate models for non-BPS 2-kink dynamics. Using these we have generated trajectories and compared the CCM dynamics with full-field dynamics. As the initial velocity increases, and as the model becomes further from BPS, the approximation gets worse, as expected. We believe the biggest problem is that the CCM model cannot radiate. Radiation is also important for a variety of other kink models, and authors have begun to incorporate radiation [40] to CCMs, although it is complicated. Our results show that radiation becomes more important as we move further from BPS theories. The results suggest that accurate CCMs of, e.g., the Skyrme model may be more difficult to construct than previously thought.

V. QUANTIZATION

In this Section, we will quantize the 1- and 2-kinks using several different quantization techniques. There are many ways to approach soliton quantization, and we will proceed using a semiclassical collective coordinate approach. Here, we define a manifold of configurations, parametrized by the coordinates $\tilde{X}_i$. We will proceed in dimensionful units, which clarifies the semiclassical approach. The classical dynamics are described by

$$\mathcal{L} = \frac{1}{2}\dot{\tilde{X}}_i \tilde{g}_{ij}(\tilde{X})\dot{\tilde{X}}_j - \tilde{U}(\tilde{X}), \tag{39}$$

where g and U are the metric and potential on the manifold. Applying a canonical quantization, we can then define a Schrödinger equation on the manifold. In the simplest approximation it is

$$\begin{aligned} &-\frac{\hbar^2}{2\tilde{g}_{\tilde{X}\tilde{X}}}\frac{d^2}{d\tilde{X}^2}\Psi + \tilde{U}(\tilde{X})\Psi = E\Psi \\ \Rightarrow\ &-\frac{\hbar^2\beta^2 m}{2g_{XX}}\frac{d^2}{dX^2}\Psi + \frac{m}{\beta^2}U(X)\Psi = E\Psi. \end{aligned} \tag{40}$$

Solutions to the Schrödinger equation are the quantum states of our problem.

To make progress using this approach, we will make three approximations.

First, we assume that paths on the collective coordinate manifold capture the true field theory dynamics. We tested this for a specific model in Sec. IV B. We saw that this approximation improves when the kink velocities are small and when μ_2 is small. The classical small velocity limit will correspond to a small momentum limit in the quantum picture.

Second, we take the weak-coupling limit. Practically, this arises from demanding that the wave function is localized in a region where the harmonic approximation can be applied [41]. One can understand the weak-coupling limit by writing the fields in the collective coordinate manifold as

$$\Phi(x;X) = \Phi_{\text{kink}}(x) + \sum_n X_n \epsilon_n(x), \tag{41}$$

and expanding in $X_n\epsilon_n(x)$. The fluctuations then satisfy a linear normal mode equation and can be calculated and manipulated easily. The normal mode equation is found by substituting (41) into (8). Neglecting the higher order terms in $X_n\epsilon_n(x)$ is equivalent to

$$\beta \ll 1, \tag{42}$$

and the μ_i of order one.

Third, the canonical quantization relies on a semiclassical approximation $\hbar \ll 1$. But note that for the quantum picture, the relevant object which appears in the Action is

$$\frac{\tilde{\mathcal{L}}}{\hbar} = \frac{m}{\beta^2\hbar}\mathcal{L}, \tag{43}$$

where $\mathcal{L}$ is the dimensionless Lagrangian [42]. Equation (43) reveals that $\hbar$ only appears with β^2. Hence for kink physics, the semiclassical limit $\hbar \to 0$ is intrinsically linked to the weak-coupling limit $\beta \to 0$.

To clarify the approximations, we write the kink energy in an approximation where the normal modes are treated harmonically, with frequencies ω_i. For more details, see Chapter 5 of [41]. The units of the harmonic correction can be read off from (40). The kink energy is

$$\frac{m}{\beta^2}\left(E_1 + \frac{1}{2}\hbar\beta^2\sum_i \omega_i + O(\hbar^2\beta^4)\right). \tag{44}$$

The mass is given by a Taylor expansion in $\hbar\beta^2$. The translational zero mode and regularization of the normal modes require more careful consideration, which we will consider later. But this formula captures the essential features of the quantum corrections. We'll now consider several quantizations in more detail.

In this section, we will keep dimensionful coordinates to better keep track of the approximations used. The quantities calculated in earlier sections, such as E_1 and E_2, remain dimensionless.

A. Reduced collective coordinate quantization

First, we will quantize using a small number of collective coordinates: just one per soliton. The 1-kink then only has one mode, the translational zero mode. As this is a zero mode, all configurations have the same energy E_1. Denoting the position as Y, the Schrödinger equation is given by

$$-\frac{m\hbar^2\beta^2}{2E_1}\partial_Y^2\Psi + \frac{m}{\beta^2}E_1\Psi = E\Psi, \tag{45}$$

with solution equal to a free particle with mass E_1,

$$E = \frac{m}{\beta^2}E_1 + \frac{\beta^2\hbar^2}{2E_1}P^2. \tag{46}$$

Here, P is the dimensionless momentum of the state. The ground state has $P = 0$ and so the quantum energy in this approximation is equal to the classical energy. This is a zero-mode quantization, which has been previously been applied to skyrmions [43], vortices [11], and monopoles [30].

The quantization of the 2-kink is more interesting as there is one nonzero mode, corresponding to the relative separation X. A similar quantization has been applied to the Deuteron [20] and the Lithium-7 nucleus [21] in the Skyrme model. Like the 1-kink case there is also a coordinate controlling the position of the center-of-mass, but this only will give rise to an overall momentum, which will be zero in the ground state. Hence we ignore this and work in the center-of-mass frame. As we have developed in the previous section, the classical Lagrangian of our collective coordinate model of two kinks takes the form

$$\tilde{\mathcal{L}} = \frac{m}{\beta^2}\left(\frac{1}{2}g(X)\dot{X}^2 - U(X)\right). \tag{47}$$

We can apply canonical quantization to find the semiclassical Hamiltonian

$$\hat{\mathcal{H}} = -\frac{\beta^2\hbar^2 m}{2}\Delta + \frac{m}{\beta^2}U(X). \tag{48}$$

Naively, the kinetic operator is just $g^{-1}\partial_X^2$, but the metric makes things more complicated: Δ is actually the Laplace-Beltrami operator. In one dimension it takes the form

$$\Delta = \frac{1}{\sqrt{g}}\partial_X\left(\frac{1}{\sqrt{g}}\partial_X\right) = \frac{1}{g}\left(\partial_X^2 - \frac{\partial_X g}{2g}\partial_X\right). \quad (49)$$

In the semiclassical approximation, bound states solve the Schrödinger equation:

$$-\frac{\beta^2\hbar^2 m}{2}\Delta\Psi + \frac{m}{\beta^2}U(X)\Psi = E\Psi. \quad (50)$$

Before solving the equation exactly, we can make an approximate solution using the harmonic approximation. Here, we ignore the first derivative term in the Laplace-Beltrami operator and approximate the potential by a quadratic. Since the potential has its minimum at a finite value, $X = X_0 \approx 2.1$, we must expand around this point, including the metric $g_0 = g(X = X_0)$. The Schrödinger equation becomes

$$-\frac{\beta^2\hbar^2 m}{2g_0}\partial_X^2\Psi + \frac{m}{2\beta^2}\omega_X^2(X - X_0)^2\Psi = E\Psi, \quad (51)$$

where ω_X is the first normal mode frequency, which can be found using the numerically generated potential $U(X)$, which we found in the previous section. Equation (51) has the ground state solution

$$\Psi \sim \exp\left(-\frac{m\omega_X(X - X_0)^2}{2\hbar}\right), \quad (52)$$

with $E = \frac{1}{2}m\hbar\omega_X/\sqrt{g_0}$. In our case, for $\mu_1 = 2$, $\mu_2 = 6.1$, the frequency is equal to $\omega_X/\sqrt{g_0} = 0.2072$. Noting that the quantum energy for the 1-kink is just the classical energy, we can calculate the quantum binding energy in the harmonic approximation. We find that

$$E_1^{\text{Harmonic}} = 10.242\frac{m}{\beta^2} \quad (53)$$

$$E_2^{\text{Harmonic}} = 19.440\frac{m}{\beta^2} + 0.1036\hbar m \quad (54)$$

$$\Rightarrow E_{\text{bind}}^{\text{Harmonic}} = (5.1 - 0.51\hbar\beta^2)\%. \quad (55)$$

The inclusion of quantum energy increases the energy of the 2-kink and so decreases the binding energy percentage, for any value of $\hbar\beta^2$. Hence quantization is an unbinding process. Note that we only trust the quantization method when $\hbar\beta \ll 1$. Hence we have not found a quantum correction which can change the sign of E_{bind}, unbinding the 2-kink.

To solve the full Schrödinger equation (50) beyond the harmonic approximation we take an initial random guess $\Psi_0(X)$ and evolve it using

$$\dot{\Psi} = -\hat{\mathcal{H}}\Psi, \qquad \Psi^2 = 1. \quad (56)$$

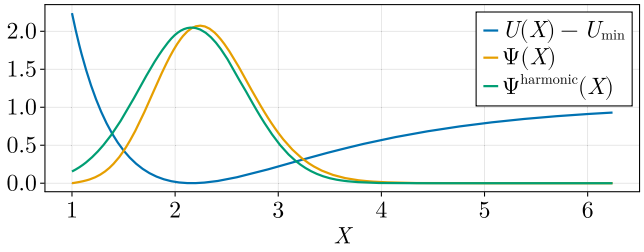

FIG. 12. The ground state wave function of the 2-kink in the collective coordinate approximation for $\mu_1 = 2$, $\mu_2 = 6.1$, in a harmonic approximation (green) and the true solution (orange). We also plot the shifted potential energy (blue).

The ground state is the late-time solution of (56). In one dimension, there is always a ground state solution. We calculate it for $\hbar = 1$, and it is shown in Fig. 12, alongside the harmonic solution. Both are concentrated near the minimum of U. The main difference between wave functions is that the boundary at the left squeezes the true wave function, moving it slightly rightwards. Due to this squeeze, the energy of the anharmonic wave function is $0.1107\hbar m$, larger than the harmonic approximation. This affects the binding energy, which is now equal to

$$\Rightarrow E_{\text{bind}}^{\text{Quantum anharmonic}} = (5.1 - 0.54\hbar\beta^2)\%. \quad (57)$$

Hence, for the same $\hbar\beta^2$, the anharmonicity has decreased the binding energy of the quantum 2-kink by a small amount.

We repeat the calculation for the near-BPS case, $\mu_1 = 2$, $\mu_2 = 4$. Here the quantum energy is $0.059\hbar m$ in the harmonic approximation and $0.053\hbar m$ in the anharmonic case. The anharmonic quantum energy is less. The percentage binding energy per kink goes from 0.80% to $(0.80 - 0.32\hbar\beta^2)\%$ for the harmonic approximation [or $(0.50 - 0.29\hbar\beta^2)\%$ in the anharmonic case]. So even though the quantum correction is smaller, the effect on the percentage binding energy is much larger.

VI. CONCLUSION AND FURTHER WORK

In this paper we have constructed a modified sine-Gordon model which supports stable static multikink solutions. Unlike usual sine-Gordon, the model is not integrable or BPS and the solutions have a binding energy. This makes the theory a good toy model for physical systems such as those found in condensed matter and nuclear theory. We believe our model is an excellent testing place for ideas in classical and quantum soliton dynamics. As such, we studied a variety of problems in the new model.

First, we calculated kink solutions for $N = 1$–20 and found that the binding energy per kink asymptotes to a constant value, similar to what is seen in nuclear matter. We then constructed a collective coordinate model of 2-kinks using pinning. This is the first time a potential and metric

have been generated on a soliton configuration space using this method. In some sense, the method is more general than that used in recent works [14], as it does not rely on features of the 1-soliton to generate approximate 2-soliton fields. We used the model to test the collective coordinate approximation for soliton dynamics against full-field theory finding that, as expected, the model works better when the model is closer to BPS. We also used the collective coordinate model to generate a quantum 2-kink solution in semiclassical harmonic and anharmonic approximations.

Overall, we calculated the binding energy three times: classically, and harmonically and anharmonically in a collective coordinate approximation. The results of these calculations are shown in Table I. The fact that the results are different highlights that the quantum binding energy is highly dependent on the method used to calculate it. In the Skyrme model, authors have calculated the binding energy classically [22], in a harmonic [26,44] and anharmonic [20] collective coordinate approach. The calculations in higher dimensions are very difficult, and so our model is an excellent tool for probing questions about quantum soliton masses in a simple setting.

There are many obvious generalizations of the work done here: one could generate collective coordinates for more than 2-kinks, calculate loop corrections [45], or ask how the binding energy calculation changes when considering more kinks. It would be interesting to add "isospin" coordinates to the model, similar to the complex sine-Gordon model [33], where solitons have additional internal symmetries. The quantization of this type of model would be closer to higher-dimensional models, which often have internal degrees of freedom. We have modified the normal sine-Gordon theory so that there are bound multikinks. But there are various other models that one could modify and study, depending on their interest.

TABLE I. Energies and binding energies using different approximations, for the 2-kink with $\mu_1 = 2$, $\mu_2 = 6.1$, and $\mu_2 = 4$. Here, we define $\tilde{\beta}^2 = \hbar\beta^2$.

$\mu_2 = 6.1$			
Method	$\frac{\beta^2}{m}E_1$	$\frac{\beta^2}{m}E_2$	$E_{\text{bind}}(\%)$
Classical	10.24	19.44	5.10
Harmonic	10.24	$19.44 + 0.10\tilde{\beta}^2$	$5.1 - 0.51\tilde{\beta}^2$
Anharmonic	10.24	$19.44 + 0.11\tilde{\beta}^2$	$5.1 - 0.54\tilde{\beta}^2$
$\mu_2 = 4$			
Classical	9.28	18.42	0.80
Harmonic	9.28	$18.42 + 0.06\tilde{\beta}^2$	$0.80 - 0.32\tilde{\beta}^2$
Anharmonic	9.28	$18.42 + 0.05\tilde{\beta}^2$	$0.80 - 0.29\tilde{\beta}^2$

ACKNOWLEDGMENTS

We thank Andrzej Wereszczyński for comments on the manuscript. C. H. thanks Kathy Hubbard for suggesting the use of a cubic spline. R. R. J. and A. N. thank the Kerala Theoretical Physics Initiative for facilitating their collaboration. C. H. is supported by the Carl Trygger Foundation through Grant No. CTS 20:25.

[1] T. Skyrme, Proc. R. Soc. A **247**, 260 (1958).
[2] T. Skyrme, Proc. R. Soc. A **262**, 237 (1961).
[3] P. Bizoń, M. Dunajski, M. Kahl, and M. Kowalczyk, Nonlinearity **34**, 5520 (2021).
[4] S. B. Gudnason and C. Halcrow, J. High Energy Phys. 08 (2022) 117.
[5] P. M. Sutcliffe, Int. J. Mod. Phys. A **12**, 4663 (1997).
[6] C. Adam and F. Santamaria, J. High Energy Phys. 12 (2016) 047.
[7] A. A. Abrikosov, J. Phys. Chem. Solids **2**, 199 (1957).
[8] X. Yu, Y. Onose, N. Kanazawa, J. H. Park, J. Han, Y. Matsui, N. Nagaosa, and Y. Tokura, Nature (London) **465**, 901 (2010).
[9] N. S. Manton, Nucl. Phys. **B150**, 397 (1979).
[10] C. H. Taubes, Commun. Math. Phys. **72**, 277 (1980).
[11] T. M. Samols, Commun. Math. Phys. **145**, 149 (1992).
[12] M. F. Atiyah and N. Hitchin, *The Geometry and Dynamics of Magnetic Monopoles* (Princeton University Press, Princeton, NJ, 2014), Vol. 11, 10.1515/9781400859306.
[13] M. F. Atiyah, N. J. Hitchin, V. G. Drinfeld, and Y. I. Manin, Phys. Lett. **65A**, 185 (1994).
[14] N. S. Manton, K. Oles, T. Romanczukiewicz, and A. Wereszczynski, Phys. Rev. Lett. **127**, 071601 (2021).
[15] F. Blaschke and O. N. Karpíšek, Prog. Theor. Exp. Phys. **2022**, 103A01 (2022).
[16] C. Adam, N. S. Manton, K. Oles, T. Romanczukiewicz, and A. Wereszczynski, Phys. Rev. D **105**, 065012 (2022).
[17] C. Adam, A. García Martín-Caro, M. Huidobro, K. Oles, T. Romanczukiewicz, and A. Wereszczynski, Phys. Lett. B **838**, 137728 (2023).
[18] E. Babaev and M. Speight, Phys. Rev. B **72**, 180502 (2005).
[19] N. S. Manton and H. Merabet, Nonlinearity **10**, 3 (1997).
[20] R. A. Leese, N. S. Manton, and B. J. Schroers, Nucl. Phys. **B442**, 228 (1995).
[21] C. J. Halcrow, Nucl. Phys. **B904**, 106 (2016).
[22] C. Adam, J. Sanchez-Guillen, and A. Wereszczynski, Phys. Lett. B **691**, 105 (2010).
[23] M. Gillard, D. Harland, and M. Speight, Nucl. Phys. **B895**, 272 (2015).
[24] C. Naya and P. Sutcliffe, Phys. Rev. Lett. **121**, 232002 (2018).

[25] F. Meier and H. Walliser, Phys. Rep. **289**, 383 (1997).
[26] S. B. Gudnason and C. Halcrow, Phys. Lett. B **850**, 138526 (2024).
[27] C. Halcrow and E. Babaev, SIGMA **19**, 034 (2023).
[28] R. Portugues and P. K. Townsend, Phys. Lett. B **530**, 227 (2002).
[29] A. Alonso-Izquierdo, M. A. G. Leon, J. M. Vaquero, and M. d. l. T. Mayado, Commun. Nonlinear Sci. Numer. Simul. **103**, 106011 (2021).
[30] B. J. Schroers, Z. Phys. C **61**, 479 (1994).
[31] D. T. J. Feist, J. High Energy Phys. 02 (2012) 100.
[32] B. Barton-Singer and B. J. Schroers, SciPost Phys. **15**, 011 (2023).
[33] F. Lund and T. Regge, Phys. Rev. D **14**, 1524 (1976).
[34] M. Peyrard and D. K. Campbell, Physica (Amsterdam) **9D**, 33 (1983).
[35] L. A. Ferreira and W. J. Zakrzewski, J. High Energy Phys. 01 (2014) 058.
[36] N. Manton and P. Sutcliffe, *Topological Solitons* (Cambridge University Press, Cambridge, England, 2004), 10.1017/CBO9780511617034.
[37] B. J. Harrington and H. K. Shepard, Phys. Rev. D **17**, 2122 (1978).
[38] D. Harland and R. Ward, Phys. Rev. D **77**, 045009 (2008).
[39] D. Harland and R. Ward, Phys. Lett. B **675**, 262 (2009).
[40] S. Navarro-Obregón, L. M. Nieto, and J. M. Queiruga, Phys. Rev. E **108**, 044216 (2023).
[41] R. Rajaraman, *Solitons and Instantons* (North-Holland, Amsterdam, 1982).
[42] S. Coleman, *Aspects of Symmetry: Selected Erice Lectures* (Cambridge University Press, Cambridge, England, 1988), 10.1017/CBO9780511565045.
[43] G. S. Adkins, C. R. Nappi, and E. Witten, Nucl. Phys. **228B**, 552 (1983).
[44] N. R. Walet, Nucl. Phys. **A606**, 429 (1996).
[45] J. Evslin, Phys. Lett. B **822**, 136628 (2021).